Research Square

Preprints are preliminary reports that have not undergone peer review.
They should not be considered conclusive, used to inform clinical practice,
or referenced by the media as validated information.

Multiphysics modeling of mode confinement, bending effects, and power overlap in silica optical fibers for high-performance photonic applications

Khan Rajib Hossain

apexlabbd2@mails.ucas.ac.cn

BGMEA University of Fashion and Technology

Md. Auria Hossain

Rajshahi University of Engineering and Technology

Khan Md Salman Adib Fuad

BGMEA University of Fashion and Technology

Muntaha Mahin

Bangladesh University of Textiles

Mir Abdul Gaffar

Bangladesh University of Textiles

Md Mehedi Hasan

University of Rajshahi

Jarin Tasnim

University of Rajshahi

M Abdul Jalil

BGMEA University of Fashion and Technology

Md Rahamatolla

BGMEA University of Fashion and Technology

Md Tajul Islam

BGMEA University of Fashion and Technology

H M Jahidul Kabir

BGMEA University of Fashion and Technology

Research Article

Keywords: Quartz glass fiber, multiphysics simulation, mode confinement, bending loss, power limit factor, COMSOL Multiphysics

Posted Date: June 19th, 2026

DOI: https://doi.org/10.21203/rs.3.rs-9958792/v1

License: This work is licensed under a Creative Commons Attribution 4.0 International License.
Read Full License

Additional Declarations: No competing interests reported.

Multiphysics modeling of mode confinement, bending effects, and power overlap in silica optical fibers for high-performance photonic applications

Khan Rajib Hossain[1,2]**, Md. Auria Hossain[3], Khan Md Salman Adib Fuad[1], Muntaha Mahin[4], Mir Abdul Gaffar[4], Md Mehedi Hasan[5], Jarin Tasnim[5], M Abdul Jalil [1*], Md Rahamatolla[1], Md Tajul Islam[1], H M Jahidul Kabir[1]

[1]Department of Natural Science, BGMEA University of Fashion and Technology, Dhaka 1230, Bangladesh.
[2]Materials Engineering, University of Chinese Academy of Sciences, Beijing, 100040, China.
[3]Department of Mechanical Engineering, Rajshahi University of Engineering and Technology, Rajshahi 6204, Bangladesh.
[4]Faculty of Textile Engineering, Bangladesh University of Textiles, Dhaka 1208, Bangladesh.
[5]Department of Applied Chemistry and Chemical Engineering, University of Rajshahi, Rajshahi 6205, Bangladesh.

****Corresponding Author Email:** apexlabbd2@mails.ucas.ac.cn (KRH), abduljalil@buft.edu.bd (MAJ)

Abstract: Quartz glass fiber is a core carrier of modern photonics and optical communication technologies. In finite-element eigenmode analysis, the influence of different fiber structures on mode-field confinement is revealed. The results show that a step-index multimode fiber with a core radius of 20 μm and a refractive index difference of 0.004 has a normalized frequency much greater than 2.4048, supporting the transmission of multiple higher-order modes, with an effective refractive index (n_{eff}) between 1.444 and 1.448. The power confinement (Γ) factor of a double-clad fiber increases significantly with the mode's effective refractive index. When n_{eff} increases from 1.4439 to 1.4478, the Γ value increases from 14.25% to 96.49%, indicating stronger core power confinement in higher-order modes, but this must be balanced against beam quality. At a bending radius of 10 cm, the mode field exhibits a significantly asymmetric distribution, the peak electric field shifts outward, and the effective refractive index decreases to 1.4498-1.4511, indicating that bending weakens the mode confinement capability. By introducing a perfectly matched layer, the leakage-mode characteristics of the microstructure fiber were successfully simulated, and the small change in the imaginary part of n_{eff} indicates the structure's high sensitivity to external disturbances. This paper establishes a unified COMSOL Multiphysics simulation framework and systematically examines the mode characteristics, power-confinement factor, and bending-loss mechanisms of step-index, double-clad, and microstructure fibers. The framework clarifies how fiber structure affects mode confinement and loss, providing a theoretical basis for optimizing next-generation fiber structures.

Keywords: Quartz glass fiber, multiphysics simulation, mode confinement, bending loss, power limit factor, COMSOL Multiphysics.

1. Introduction

The development of fiber optic communication began in the 19th century. In 1840, John Tyndall experimentally demonstrated that light could propagate through curved media (such as water or glass), laying the foundation for the principles of fiber optics. In 1950, Narinder Singh Kapany systematically developed fiber-optic technology and proposed the term "fiber optic," earning him the title of "father of fiber optics." In 1966, Charles K. Kao pointed out that high-purity silica glass could significantly reduce optical signal attenuation, laying the theoretical foundation for modern fiber optic communication and thus being hailed as the "father of fiber optic communication." In 1970, Robert Maurer and Peter Schultz of Corning Glass Works successfully fabricated low-loss silica glass optical fibers using vapor deposition technology, solving a key technical problem [1]. In 1977, fiber optics was first used in the Chicago telephone communication system, with one fiber replacing 261 pairs of copper wires. Compared to copper wires, fiber-optic data transmission capacity is approximately 65000 times higher. In practical communication, 1310 nm is typically used for transmission (upstream) and 1550 nm for data transmission (downstream) to achieve low-loss, high-efficiency operation [2]. Quartz glass optical fibers, with their excellent transmission efficiency, mechanical stability, and thermal stability, have become the core carrier of modern photonics and optical communication technologies [3]. In the design and application of fiber-optic devices, optical coupling characteristics directly determine the system's energy transmission efficiency and signal quality, and serve as key indicators for evaluating fiber performance. As fiber lasers, sensors, and high-power transmission systems advance toward integration and extreme-environment applications, a deep understanding and precise control of the mode field distribution, loss mechanisms, and multiphysics coupling effects within the fiber have become a current research focus. In recent years, researchers have conducted extensive work on structural innovations in optical fibers [4]. In the field of microstructure fibers, Ma et al. [5] designed and fabricated a narrow-diameter polarization-maintaining photonic crystal fiber. By optimizing the number of air-hole layers and hole spacing, they achieved a high birefringence of 8×10^{-4} and a low confinement loss of 1.32×10^{-9} dB/m at 1550 nm, providing a new technical solution for high-precision miniature fiber-optic gyroscopes. Zhang et al. [6] proposed a broadband large-mode-area double-clad photonic crystal fiber structure and systematically analyzed the effective mode area and confinement loss at different wavelengths. The results showed that the structure achieved a mode area of 731.26 μm^2 at 1.55 μm and a confinement loss of only 1.58×10^{-8} dB/m, demonstrating its potential for high-power laser transmission. In the field of hollow-core fiber, Liu et al. [7] reported an ultra-low-loss hollow-core antiresonant fiber. By introducing a straight-rod structure within a nested circular tube, they reduced the confinement loss to 1.31×10^{-7} dB/m at 1550 nm and maintained a bending loss below 8.02×10^{-5} dB/m for bending radii greater than 5 cm, significantly outperforming traditional structures. Simović et al. [8] conducted research on W-type microstructure plastic fibers and showed that by using a

gradient refractive-index-core design and a double-clad structure, the coupling length required for mode equilibrium distribution can be effectively shortened, thereby significantly improving fiber bandwidth and making it suitable for short-distance high-speed communication scenarios. However, despite the significant progress made in optimizing single performance indicators, several key research gaps remain to be explored. First, the mechanism of bending-induced optical loss is not fully elucidated. Bending not only leads to mode-field distortion and an asymmetric distribution but also induces mode leakage and an effective refractive-index drift. Especially at small bending radii, the differences in loss mechanisms between conventional step-index fibers and the bending resistance of microstructure fibers warrant systematic comparison. Gopalakrishnan et al. [9] pointed out that leakage modes in microstructure fibers often exhibit fine field distribution characteristics, requiring high-precision adaptive algorithms to accurately capture their loss characteristics. The power-confinement capability in double-clad and microstructure fibers is a key factor affecting the efficiency of fiber amplifiers and lasers. Existing research mainly focuses on mode-field-area or confinement-loss analysis under a single structural parameter, lacking a systematic exploration of how the power-confinement factor varies with mode order, refractive-index difference, and cladding geometry [10]. Gan et al. [11] showed that in extreme environments, such as pulsed plasma radiation, thermo-optical and photoelastic effects in fibers dynamically alter the refractive index distribution, leading to phase drift and additional loss. This multi-physics coupling problem is often overlooked in conventional fiber modeling.

This paper aims to establish a unified COMSOL Multiphysics simulation framework to systematically study the mode characteristics, power-confinement factor, and bending-loss mechanisms in step-index fibers, double-clad fibers, and microstructure fibers. Through finite-element characteristic mode analysis, the influence of various optical effects on mode confinement is revealed, with a focus on mode field distortion under bending perturbations, stress-optical coupling, and the interaction of thermo-mechanical-optical multiphysics fields. The research results will provide a theoretical basis and numerical support for the structural optimization and engineering applications of next-generation bend-resistant, high-power, and high-sensitivity optical fibers.

2. Fiber structures and modeling parameters

2.1 Step-index fiber geometry

Step-index fiber consists of a high-refractive-index core and a low-refractive-index cladding. The light wave is confined to the core for propagation through total internal reflection [12]. In this study, a two-dimensional axisymmetric model was established using COMSOL Multiphysics. The optical signal is confined to the core region through total internal reflection. The core radius was set to 20 μm, the cladding radius to 62.5 μm, and

the working wavelength to λ = 1.55 μm (**Figure 1**). In terms of material parameter settings, the refractive index of the pure silica core was n_{core}=1.448, the refractive index of the doped silica cladding was n_{clad}=1.444, and the refractive index difference Δn=0.004. According to the official COMSOL documentation, with these parameter settings, the effective refractive index n_{eff} of the fundamental mode lies between the core and cladding refractive indices, and the mode field is mainly concentrated in the core region. The mesh was refined using physical field control to ensure the analytical accuracy of the field distribution at the boundary. Yadgeer et al. [13] used the COMSOL frequency-domain electromagnetic wave interface to perform mode analysis of silica fibers with different refractive indices, verifying the platform's reliability in calculating the effective mode refractive index and dispersion characteristics. Their calculation results showed an error of less than 7% compared to theoretical values.

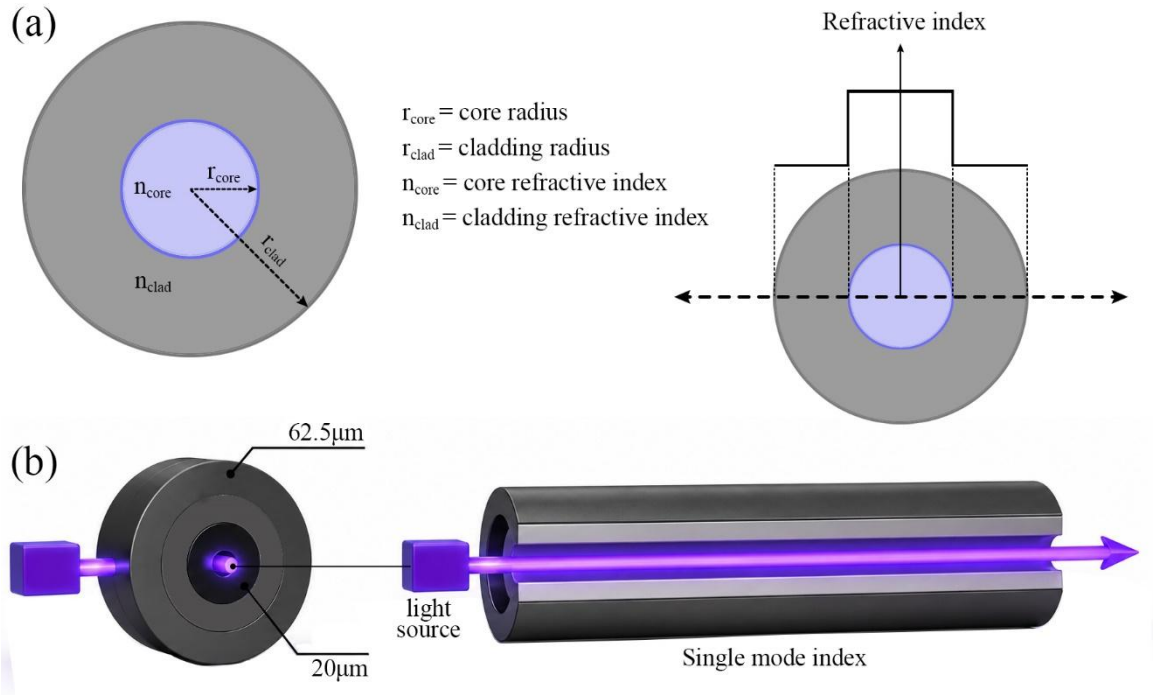


Figure 1. Schematic diagram of (a) the cross-sectional structure and refractive index distribution of a step-index single-mode fiber, and (b) a three-dimensional model of a single-mode fiber and its optical transmission path, wherein the core radius is 20 μm, and the cladding radius is 62.5 μm.

2.2 Microstructure fiber design

Microstructure fibers (MFs) typically consist of a single silica material and periodically arranged air holes. The high refractive-index contrast between the air holes and the silica substrate enables flexible dispersion control and mode-field confinement [14]. Air hole lattice arrangement, a typical structure uses a triangular lattice, with aperture diameter (d)

and spacing (Λ) as key geometric parameters (**Figure 2**). Li et al. [15] designed a variable-aperture photonic crystal fiber, employing the full-vector finite element method (FVFEM) combined with anisotropic perfectly matched layer (APML) boundary conditions. They achieved ultra-flat dispersion of 0 ± 0.68 ps/(nm·km) in the 1.25-1.78 μm wavelength range, with a confinement loss below 10^{-3} dB/m. By adjusting the size and arrangement of the air holes, the effective refractive index curve of the mode can be finely controlled, achieving dispersion compensation or nonlinear optimization. Hou et al. [16] reported that changes in the d/Λ ratio significantly affect the mode's effective refractive index and dispersion characteristics; a ±2% fluctuation in structural parameters can lead to a significant shift in dispersion compensation performance. Tenderenda et al. [17] demonstrated that large air holes near the fiber core introduce significant compressive stress in the fiber core region, thereby altering the fiber's strain-induced effective refractive index response, providing a new approach for fiber-optic sensing design.

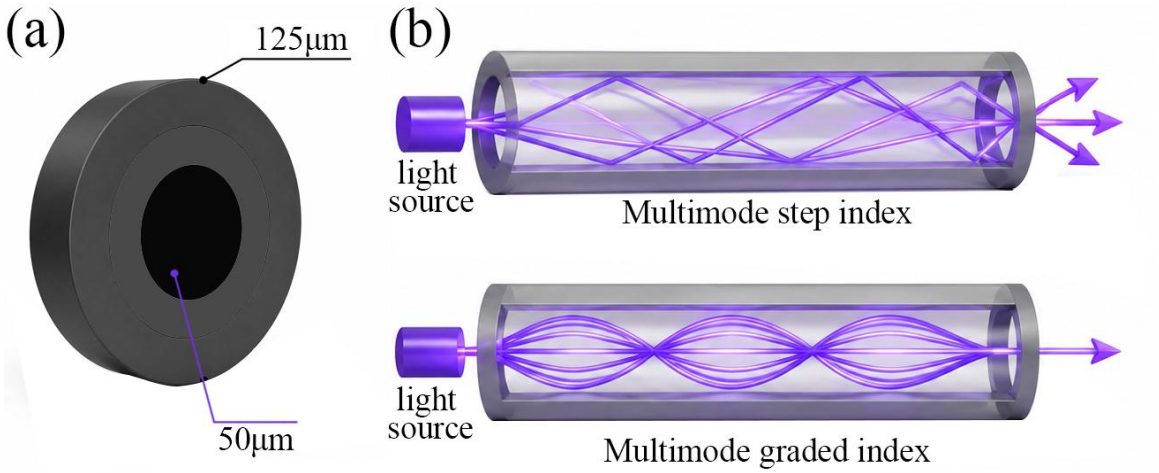


Figure 2. (a) Schematic diagram of the cross-sectional structure of a multimode step-index fiber, and (b) Comparison of light propagation paths in multimode step-index and multimode graded-index fibers, where the core diameter is 50 μm, and the cladding diameter is 125 μm.

2.3 Material properties

The step-index fiber model established in this study uses doped silica glass as both the core and cladding materials. It is physical and thermomechanical parameters significantly influence the fiber's mode stability and environmental adaptability. The thermo-optic coefficient of silica is approximately 1.0×10^{-5} K^{-1}, indicating that temperature changes alter the refractive index, thereby affecting the effective refractive index and the mode propagation constant [18]. This effect is particularly critical for high-precision sensing and temperature-sensitive devices at a working wavelength of 1.55 μm. Its elastic modulus is approximately 70-73 GPa, and its Poisson's ratio is approximately 0.16-0.17, demonstrating good mechanical stiffness and structural stability, which is beneficial for maintaining the geometric integrity of the core-cladding interface [19]. Furthermore, quartz

has a thermal conductivity of approximately 1.38 W/(m·K) and a coefficient of linear expansion of approximately 5.5×10^{-7} K^{-1}, exhibiting high thermal stability that effectively reduces the disturbance to mode distribution caused by thermal stress. These material parameters ensure stable mode propagation performance of optical fibers under thermo-mechanical coupling environments. [20]

4. Results and discussion

4.1 Mode profiles and effective Index

Based on finite-element eigenmode analysis, the mode-field distribution and corresponding effective refractive index (n_{eff}) of optical fibers with different structures can be obtained. The effective refractive index typically satisfies $n_{clad} < n_{eff} < n_{core}$, and its value reflects the degree of mode constraint on the fiber core. For the aforementioned structural parameters (r_{core} = 20 μm, n_{core} = 1.448, n_{clad} = 1.444, λ_0 = 1.55 μm), the calculated n_{eff} is close to the core refractive index, indicating that the core region mainly constrains the modes. Compared to graded-index fibers, step-index multimode fibers have more pronounced mode boundaries and significant abrupt changes in the field gradient at the interface. Single-mode structures exhibit high mode purity and strong transmission stability, while multimode structures offer greater tolerance to core diameter variations and stronger structural adaptability [21]. Therefore, differences in mode distribution and effective refractive index directly determine the application direction of optical fibers in communication, sensing, and high-power transmission. Doped silica glass is used as the material. The refractive index difference between the core and cladding is achieved by changing the doping concentration [22]. Since $n_{core} > n_{clad}$, the total internal reflection condition is satisfied, thus achieving effective confinement of light in the core. Simulation results show that the electric field is mainly confined to the core region and rapidly attenuates into the cladding at the interface, exhibiting typical step-index fiber guiding mode characteristics. The normalized frequency (V-number) of a step-index fiber is defined as equation (1). [23]

$$V = \frac{2\pi r_{core}}{\lambda_0}\sqrt{n_{core}^2 - n_{clad}^2} \quad \text{---------- (1)}$$

Calculations show that $V \gg 2.4048$ (the first zero of the Bessel function J_0), therefore, this structure belongs to a multimode fiber. Theoretically, when $V < 2.4048$, only linearly polarized 01 (LP_{01}) fundamental mode propagation is supported (single-mode). When $V > 2.4048$, multiple higher-order modes are supported (multi-mode). COMSOL eigenmode solution results show an effective refractive index, n_{eff} = 1.4458, between n_{core} and n_{clad}, consistent with the guided mode's physical characteristics. The field distribution plot shows a clear radial oscillation structure, further verifying its multimode operation. This study employs an ideal step refractive index profile model equation (2). [24]

$$n(r) = \begin{cases} n_{core}, & r \le r_{core} \\ n_{clad}, & r_{core} < r \le r_{clad} \end{cases} \quad \text{---------- (2)}$$

The model exhibits abrupt changes at the core-cladding interface, forming a significant refractive index step (Δn = 0.004) [25]. The electric field intensity distribution diagram shows that the core region is a high-field-intensity region, the cladding field intensity decreases exponentially, and a significant change in field gradient occurs at the interface. This abrupt refractive index structure is the primary cause of modal dispersion in multimode step-index fibers [26]. Compared to graded-index fibers, its group velocity difference is greater, making it more suitable for short-distance or high-power transmission applications. In this model, the cladding radius is 62.5 μm, much larger than the core radius. The larger cladding size effectively reduces the impact of boundary reflections on the guided mode, decreases boundary perturbations in numerical calculations, and improves the stability of the mode field. Simulation results show that the electric field is significantly attenuated near the outer boundary of the cladding, indicating that the cladding thickness is sufficient to ensure the mode is completely confined within the core region (**Figure 3**). The arrow diagram further reveals the direction of the electric field vector, showing that the electric field distribution exhibits radial symmetry, consistent with the predictions of LP mode theory. [27]

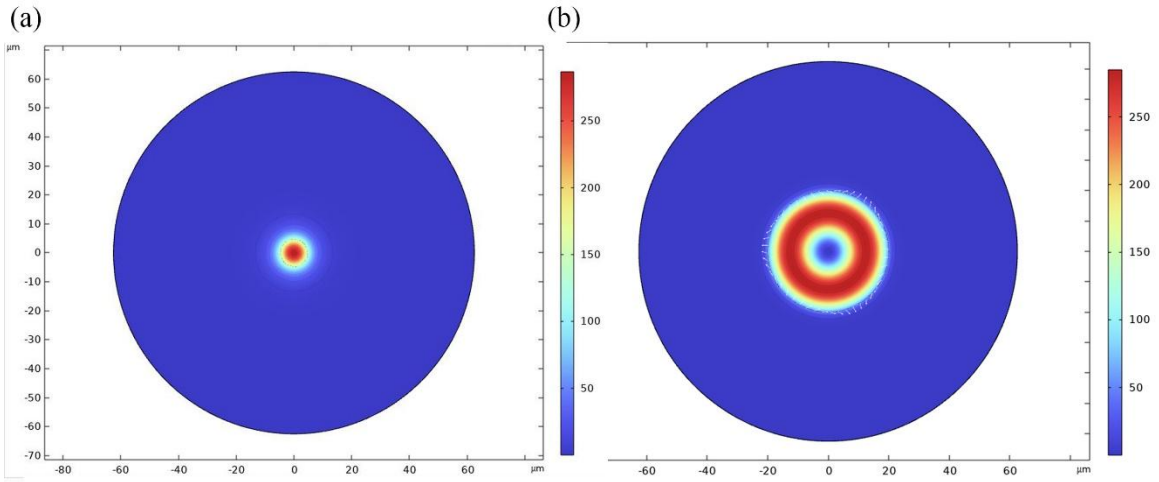


Figure 3. Finite element mode field distribution and effective refractive index characteristics of (a) single step-index fiber structure and core/cladding distribution, and (b) multimode step-index fiber, demonstrating the constraint and propagation behavior of the optical field in the fiber core.

Finite element eigenmode analysis based on COMSOL Multiphysics shows that the established step-index doped silica fiber structure has stable guided mode characteristics. The effective refractive index lies between the core and cladding refractive indices, as required by waveguide theory. The normalized frequency is much greater than 2.4048, verifying that it is a typical multimode fiber. The electric field at the interface exhibits obvious step-index constraint characteristics. The structural parameters (20/62.5 μm, Δn=0.004) are similar to those of standard communication-grade multimode silica fiber, providing a reliable numerical basis for subsequent bending-loss analysis, mode-coupling research, and structural optimization. This study used COMSOL Multiphysics to perform eigenmode analysis of silica-doped glass optical fibers, focusing on the spatial distributions

and vector-field characteristics of the electric and magnetic fields. The fiber structure includes a core and a cladding, with the core and cladding radii set to predetermined values (based on the simulation model). The Maxwell equations were solved using the finite element method to obtain the distribution maps of the electric field component E_z and the magnetic field component H_z of the modes. **Figure 4** shows the surface distribution of the z-component of the electric field (E_z) for different effective mode indices. The RainbowLight color table is used to visualize the electric field intensity; red to yellow areas represent regions with higher electric field intensity, while blue to purple areas correspond to lower values. The figures show that the electric field is mainly concentrated in the core region, exhibiting typical guided mode distribution characteristics, indicating that light energy is effectively confined within the core for propagation.

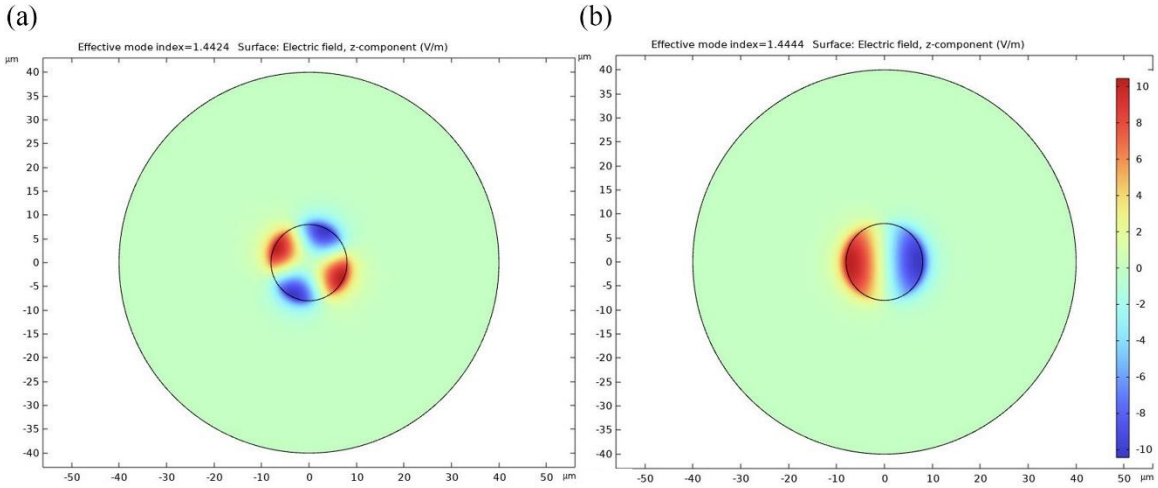


Figure 4. (a) shows the operating wavelength λ = 1.4424 μm, (b) shows λ = 1.4444 μm. The electric field is mainly localized in the core region, exhibiting obvious step-index constraint characteristics at the core-cladding interface, indicating that the structure supports stable guided mode propagation, consistent with the typical waveguide characteristics of multimode fibers.

To further reveal the field's vector direction, **Figure 5** shows a superimposed contour map of the electric field z-component (E_z) and the magnetic field z-component (H_z). In this figure, the electric field is represented by surface coloring, while the magnetic field is presented as 20 contour lines. The orthogonality of the electric and magnetic fields is clearly shown, consistent with the fundamental laws of electromagnetic wave propagation in a medium. The magnetic field contour lines are densely distributed at the core-cladding interface, reflecting drastic changes in magnetic field intensity in this region, possibly related to boundary conditions and differences in the refractive index of the medium. By comparing the field distributions for different effective mode indices, it was found that the effective refractive index of the mode significantly affects field confinement. Higher effective mode indices correspond to stronger field localization, further verifying the modulating effect of fiber structure parameters on mode characteristics. The COMSOL

Multiphysics simulation platform provides an intuitive, accurate tool for analyzing the electromagnetic field distribution in silica-doped glass fibers. The vector visualization of the electric and magnetic fields deepens understanding of mode behavior in optical waveguides and provides a theoretical basis for the optimized design of fiber-optic devices.

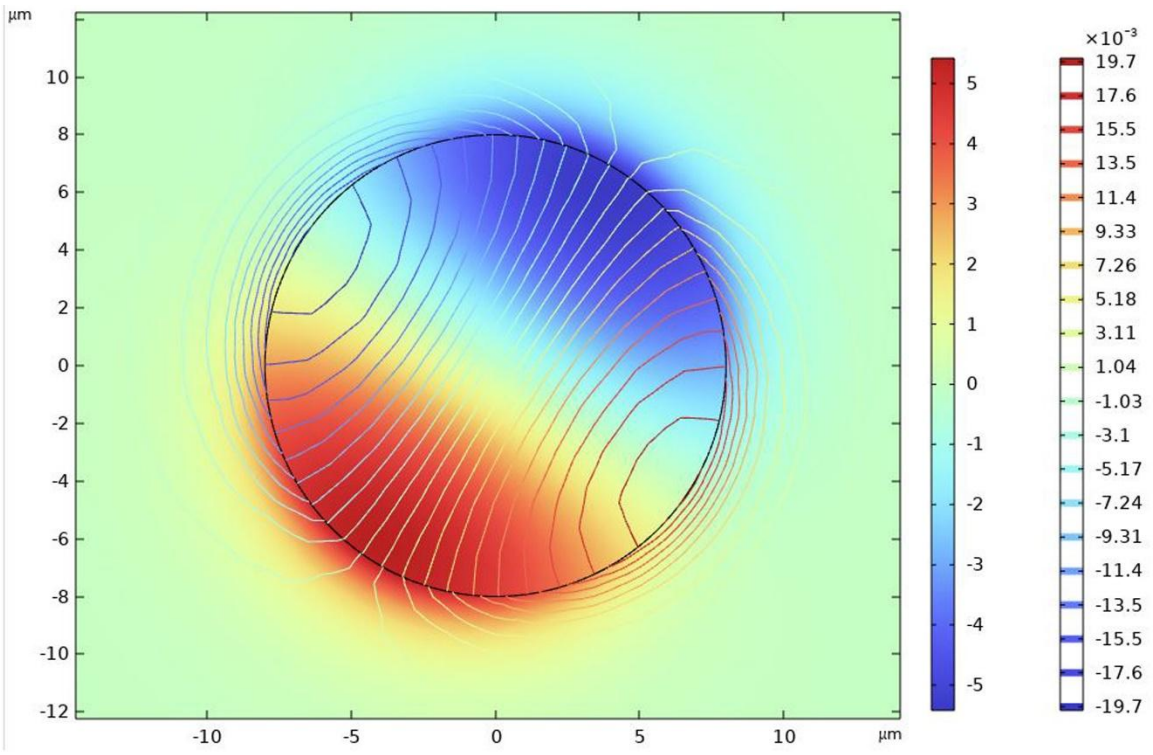


Figure 5. The superposition distribution of the z-components (Ez) of the electric field and the z-components (Hz) of the magnetic field reveals the orthogonality of the mode fields and the field constraint characteristics of the core-cladding interface.

4.2 Power confinement and overlap factor

Mode analysis of the double-clad fiber was performed using COMSOL Multiphysics software, yielding the electric field distribution of the fundamental mode. Simulation results show that at 1550 nm, the effective refractive index of the supported modes is 1.4439, and the electric field is mainly concentrated in the core region, exhibiting the typical fundamental mode field distribution. The power confinement factor is an important parameter for measuring the degree of overlap between the optical field and the gain medium (such as a rare-earth-doped fiber core). In this simulation, we calculated the power confinement factor for different modes by integrating the power in the core region to the total power. As shown in **Table 1**, the power confinement factor exhibits significant differences with varying mode order. For the fundamental mode (effective refractive index 1.4439), the power confinement factor is approximately 0.142, indicating that only about

14.2% of the optical power is confined in the fiber core. As the effective refractive index of the mode increases, the power confinement factor gradually rises, reaching a maximum of 96.49% (e.g., for higher-order modes with an effective refractive index of 1.4478). This trend indicates that higher-order modes have stronger power confinement capabilities in the fiber core, which is related to the higher field intensity distribution of higher-order modes in the core region. Double-clad fiber, due to its unique inner and outer cladding structure, can effectively confine pump light in the inner cladding while maintaining signal light transmission in the fiber core [28]. The refractive index distribution used in the simulation is a typical step-index structure, with the core refractive index slightly higher than that of the inner cladding and the inner cladding refractive index higher than that of the outer cladding. By comparing the power-limiting factor across different structural parameters, we found that as the refractive index difference between the core and the inner cladding increases, the power-limiting factor of the fundamental mode improves significantly. Increasing the inner cladding diameter reduces the overlap efficiency between the signal and pump beams, thus affecting the amplifier's gain performance. The core diameter has a relatively small impact on the power-limiting factor but significantly affects the mode-field distribution and single-mode conditions [29]. These results emphasize that in a double-clad fiber design, the refractive index difference and the matching between the core and inner cladding diameters must be considered comprehensively to achieve efficient light-matter interaction and good beam quality.

The simulation was performed using COMSOL Multiphysics, employing the electromagnetic wave frequency-domain (ewfd) interface for mode analysis. At a wavelength of 1.5500 μm, the calculated effective mode index was 1.4439, corresponding to the propagation constant of the fundamental mode. The electric field norm distribution is shown in **Figure 6**, illustrating the distribution of the optical field in the fiber core region. The core advantage of double-clad fiber lies in its ability to guide high-power pump light through the inner cladding while maintaining efficient signal light propagation within the fiber core. Simulation results in this study show that higher-order modes corresponding to high power limiting factors (>80%) can improve gain efficiency and introduce the risk of beam quality degradation. In silica glass optical doped fiber lasers, mode selection, doping distribution, and refractive index difference should be comprehensively considered to achieve a balance between high efficiency and good beam quality. The power limiting factor should be considered a key indicator in fiber design, especially in high-power applications, as it directly affects the laser's slope efficiency and thermal management requirements.

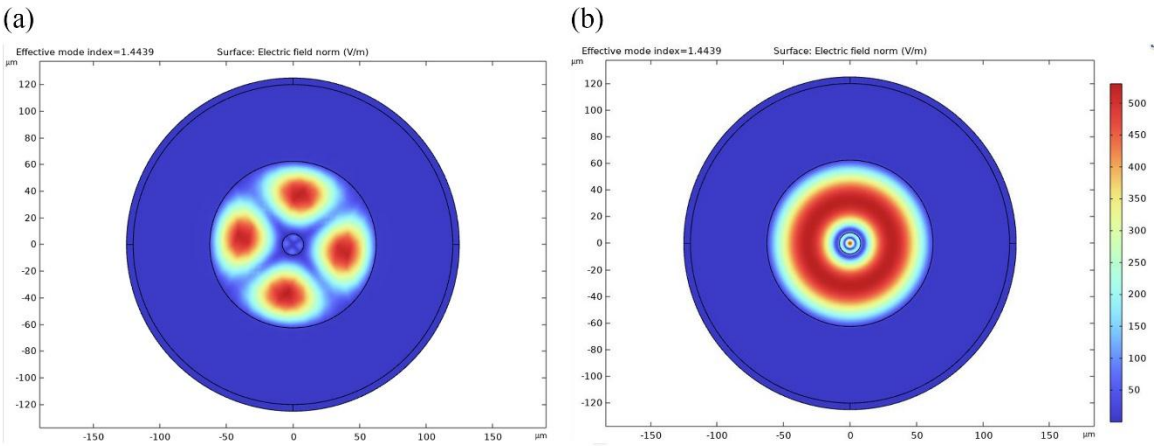


Figure 6. Mode field distribution and optical field overlap characteristics of double-clad fiber: (a) Power confinement factor distribution when n_{eff} = 1.4439, and (b) Optical field overlap factor distribution between the core and the first cladding (Clad 1) when n_{eff} = 1.4439.

The data in the **table 1** clearly show that the power confinement factor increases significantly with increasing effective mode index. When the effective refractive index is 1.4439, the Γ value is only 0.14246 (approximately 14.25%), indicating that the optical field distribution of this mode is relatively diffuse, with only a small amount of power concentrated in the fiber core. When the effective refractive index rises to 1.4455, the Γ value increases to approximately 78%, indicating that the optical field is more tightly confined to the fiber core. When the effective refractive index reaches 1.4497, the Γ value approaches 96.49%, demonstrating extremely high power confinement capability. This trend indicates that higher-order modes (or modes closer to the fiber core refractive index) exhibit greater power confinement in the fiber core, which is of great significance for improving the gain efficiency of fiber amplifiers or lasers.

Table 1. Power confinement factor and effective mode index of supported modes in the double-clad fiber.

Effective mode index	Wavelength in free space (μm)	P_core (W)	P_full (W)	Power Confinement (1)
1.4439	1.55	1.10E-09	2.66E-06	0.0414
1.4439		1.26E-09	3.05E-06	0.0413
1.4439		9.46E-05	6.64E-02	0.1425
1.4439		2.45E-09	1.76E-06	0.1391
1.4439		2.41E-09	1.73E-06	0.1390
1.4439		6.86E-10	5.03E-07	0.1365
1.4439		2.94E-09	6.49E-07	0.4537
1.4439		2.94E-09	6.48E-07	0.4535
1.4449		4.94E-09	7.42E-09	66.4990
1.4449		5.17E-09	7.77E-09	66.5029
1.4455		4.86E-09	6.23E-09	77.9891
1.4455		4.93E-09	6.32E-09	77.9933
1.4455		5.49E-09	7.05E-09	77.9445

1.4455		5.85E-09	7.51E-09	77.9461
1.4478		5.60E-09	6.23E-09	89.9306
1.4478		9.01E-09	1.00E-08	89.9583
1.4478		9.05E-09	1.01E-08	89.9611
1.4478		7.99E-04	8.88E-04	89.9488
1.4497		2.40E-08	2.49E-08	96.4925
1.4497		2.31E-08	2.39E-08	96.4933

4.3 Bending-induced effects

To investigate the electromagnetic field distribution in optical fibers under bending conditions, a two-dimensional axisymmetric electromagnetic wave frequency-domain (ewfd) model was established in COMSOL Multiphysics. The simulation parameters were set as follows: bending radius (r_{bend}) 10 cm, core diameter (r_{core}) 20 μm, cladding diameter (r_{clad}) 62.5 μm, core refractive index (n_{core}) 1.451, cladding refractive index (n_{clad}) 1.444, operating wavelength (λ) 1.55 μm. The effective refractive index calculations show that, under bending, the fundamental mode's effective refractive index varies slightly between approximately 1.4498 and 1.4511. This indicates that bending introduces an additional equivalent refractive-index perturbation, leading to a shift in the mode propagation constant. As the bending effect intensifies, the mode field gradually shifts outward, resulting in a significant asymmetric field distribution. Under a bending radius of 10 cm, the electric field intensity distribution within the fiber cross-section clearly concentrates outward from the bend. The peak electric field gradually shifts outward from a symmetrical distribution. The field distribution within the core region gradually evolves from an initial approximately symmetrical Gaussian distribution to an eccentric distribution. The field intensity is enhanced at the outer interface and weakened at the inner interface. This distribution characteristic indicates that bending generates an equivalent transverse stress gradient and refractive index perturbation, leading to a redistribution of mode energy. The reduced equivalent refractive index outside the bend causes the mode field to be "stretched" in that direction, resulting in a significant stress-optical coupling effect (**Figure 7**). The following trends can be observed from the electric field mode distribution diagram: under small bending perturbations, the modes maintain their quasi-fundamental mode shape but exhibit slight eccentricity; as the bending effect intensifies, the mode field shape evolves from a circularly symmetric structure to an elliptical or unilaterally enhanced structure; a weak leakage field distribution appears in the cladding region, indicating radiation loss. The slight decrease in the effective refractive index and the extension of the mode field into the cladding indicate that bending weakens mode confinement, resulting in bending loss. Energy gradually couples to the cladding and even radiates into the external medium, leading to mode distortion and asymmetric enhancement of the field strength. As seen in the figure, when the field strength is significantly concentrated on the outside of the bend, the mode no longer maintains the ideal LP01 symmetric structure but instead exhibits a single-peak shift characteristic. This distortion is an important precursor to bending loss.

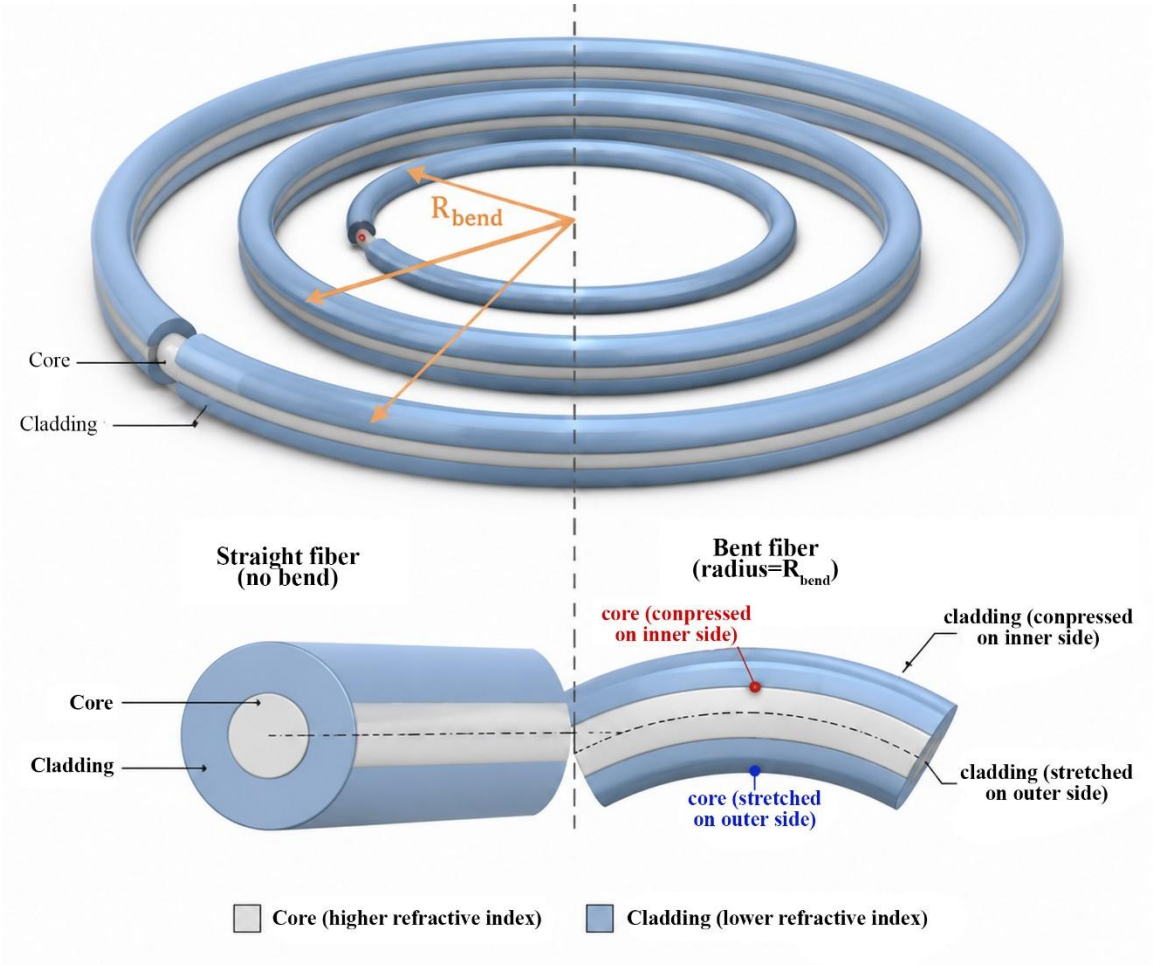


Figure 7. A schematic diagram of an optical fiber bending structure and its effect on core-cladding geometry and refractive index distribution, where the bending radius is R_{bend}.

Compared to conventional step-index fibers, microstructured fibers (such as air-hole-cladding structures) typically exhibit stronger lateral mode confinement. Under the same bending radius (10 cm), Conventional optical fibers are more prone to mode field shift and leakage; the effective refractive index changes more significantly; and a larger leakage field distribution appears in the cladding. Microstructured optical fibers, due to their high refractive-index contrast and structural confinement, can significantly reduce bending-induced loss and improve bending resistance. Therefore, under the 1.55 μm communication band conditions, the results of this study show that in conventional single-mode optical fibers with a core diameter of 20 μm and a cladding of 62.5 μm, a bending radius of 10 cm already causes considerable mode shift and field distribution distortion; in contrast, microstructured optical fibers exhibit superior mode stability and bending resistance under the same conditions. Based on COMSOL numerical simulations, we conclude that bending results in a slight decrease in the effective mode refractive index. The mode field

concentrates towards the outer side of the bend. A leakage field distribution appears in the cladding. The mode distribution gradually transforms from a symmetrical distribution to an asymmetrical distortion structure. The above results systematically reveal the mechanism by which bending affects the electromagnetic field distribution and propagation characteristics of optical fibers, providing a theoretical basis for optimizing the design of bending-resistant optical fiber structures **(Figure 8)**.

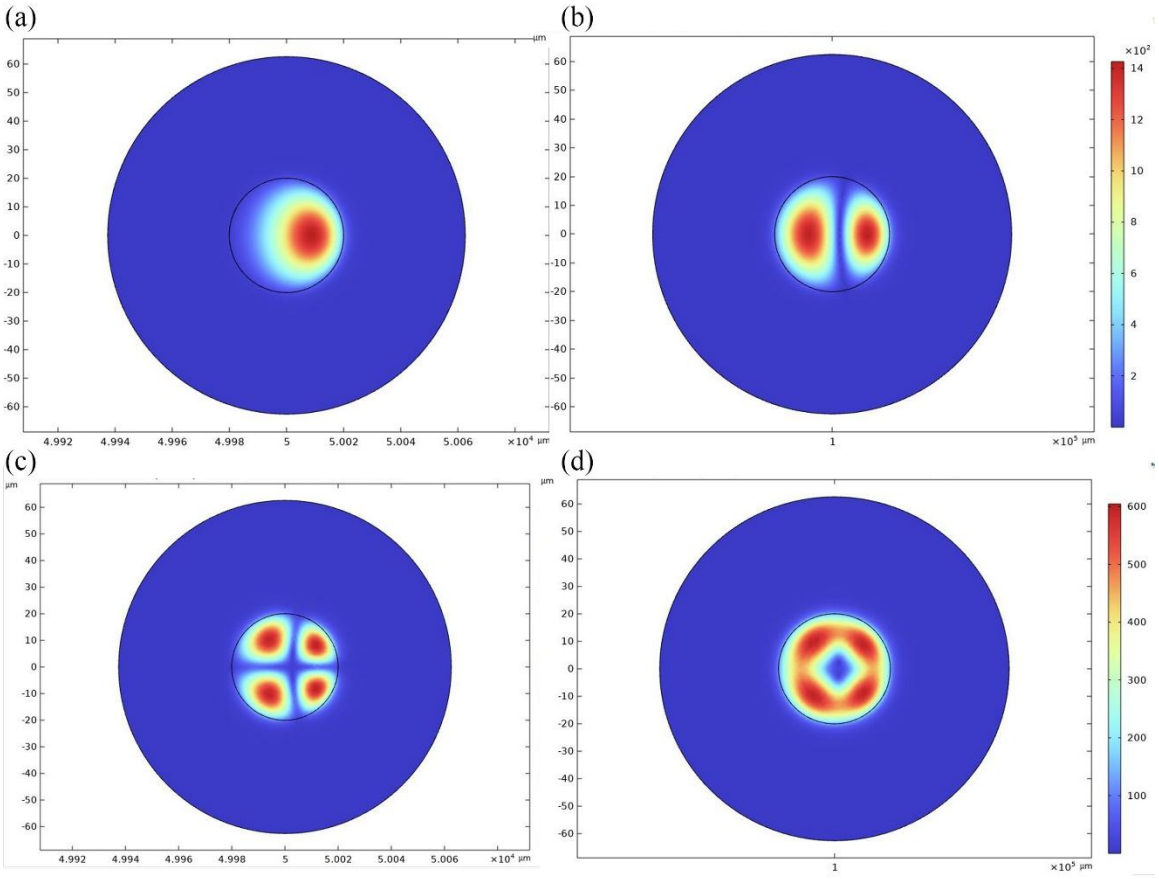


Figure 8. (a) Electric field distribution of a conventional step-index fiber at a bending radius of 10 cm, with the mode field shifting outwards, (b) Asymmetric mode field of a conventional bent fiber, with enhanced cladding leakage, (c) Bending mode distribution of an air-hole microstructured fiber, showing better bending stability, and (d) Mode field in a microstructured fiber is confined near the core region, exhibiting strong lateral constraint.

4.4 Multiphysics interaction analysis

This study constructs a two-dimensional finite element model of a microstructured optical fiber and analyzes its mode characteristics, leakage loss, and sensitivity to external disturbances. Model parameters include: aperture radius r_{hole} = 2.5 μm, aperture spacing Δ = 6.75 μm, fiber radius r_{fiber} = 10 μm, background refractive index n_{bg} = 1.45, air refractive index n_{air} = 1, and operating wavelength λ_0 = 1.45 μm. To accurately capture the leakage

mode, a perfectly matched layer (PML) and a scattering boundary condition (SBC) were used [30]. The PML thickness was set to

$$\lambda_T = \lambda_0 / \sqrt{n_{bg}^2 - n_{eff,max}^2} \quad \text{---------- (3)}$$

where n_{eff},Max=1.4454 and n_{eff},Min=1.429.

Figure 9b show the electric field distribution at effective refractive indices n_{eff} = 1.4304-2.1612 × 10^{-5i} and n_{eff} = 1.4304-1.9981 × 10^{-5i}. In both modes, the electric field is mainly concentrated in the fiber core, demonstrating strong mode confinement. The small imaginary part indicates that the structure has low leakage loss at the target wavelength. The PML setting effectively absorbs the radiated energy, improving the accuracy of leakage loss extraction. **Figure 9c** shows the distribution characteristics of the magnetic field components $|H_z|$ and $|H_y|$. The axial component $|H_z|$ exhibits a symmetrical distribution in the fiber core region, indicating good axial confinement and conforming to the typical characteristics of a hybrid mode (HE/EH). The transverse component $|H_y|$ exhibits significant asymmetry and localized field enhancement around the air holes, reflecting the modulation effect of high refractive index contrast on the magnetic field distribution. Combined with the imaginary part of the effective refractive index (1.9981 × 10^{-5}), the mode exhibits low leakage loss and no significant outward radiation of the magnetic field distribution, verifying the effectiveness of the PML boundary. Furthermore, $|H_y|$ is more sensitive to refractive index perturbations and can serve as a key indicator for evaluating the fiber's response to external thermal coupling perturbations.

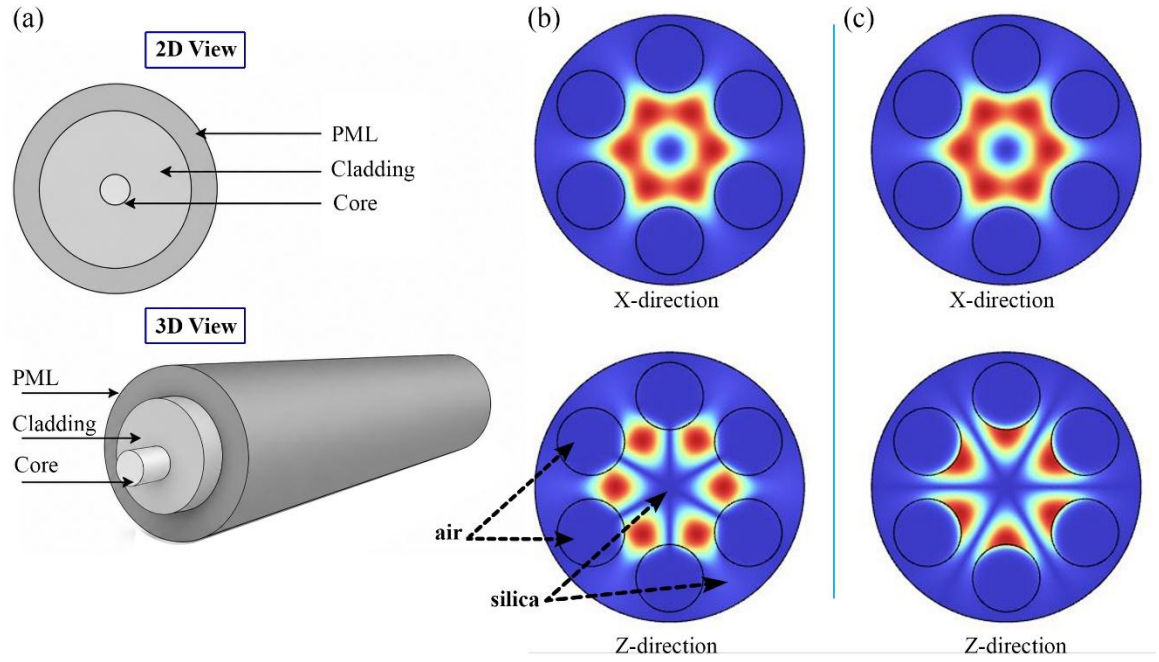


Figure 9. (a) Schematic diagram of photonic crystal fiber structure, showing 2D cross-section and 3D view, with the fiber core, cladding and perfect matching layer (PML) labeled, (b) Electric field distribution in the X and Z directions, with the real part concentrated in the fiber core and the imaginary part extremely small, indicating that the mode has low leakage loss and the PML effectively absorbs radiated energy, and (c) Characteristics of magnetic field distribution in the X and Z directions, with |Hz| symmetrically distributed in the core, showing good axial constraint, and |Hy| locally enhanced and asymmetrical around the air holes, reflecting the modulation effect of high refractive index contrast on the magnetic field, and sensitive to refractive index perturbations, which can be used to evaluate the fiber's response to external thermal perturbations.

In real-world operating environments, fiber performance is affected by the coupling of thermal and mechanical fields. Temperature variations cause fluctuations in the material's refractive index (thermo-optic effect) and structural expansion (thermal expansion effect), thereby altering the mode's effective refractive index and shifting phase-matching conditions, introducing additional losses. Furthermore, mechanical stresses (such as bending, tension, or pressure) can induce asymmetric changes in the refractive index distribution via the elasto-optic effect, thereby affecting the mode's polarization state and leakage characteristics [31]. This model, by introducing PML and SBC boundary conditions, can simulate the amplification effect of these perturbations on mode leakage, providing a theoretical basis for fiber design under multiphysics coupling. The sensitivity of optical fibers to external disturbances is mainly reflected in the changes in the real and imaginary parts of the effective refractive index. By comparing the mode distribution under different disturbance conditions, the response characteristics of optical fibers in sensing applications can be evaluated. In this study, the change in the imaginary part of n_{eff} (from 2.1612×10^{-5} to 1.9981×10^{-5}) indicates that even small disturbances can significantly affect leakage loss, reflecting the high disturbance sensitivity of this structure. By combining the multiple boundary conditions and composite image analysis method described in Figure 3, this study provides a quantitative analysis method for the disturbance response mechanism of microstructured optical fibers in high-sensitivity applications such as sensing and communication.

5. **Conclusions**

This paper establishes a unified multiphysics simulation framework for silica glass fibers in COMSOL Multiphysics and systematically studies the mode characteristics, power-limiting factor, and bending-loss mechanism of step-index, double-clad, and microstructure fibers. Through finite-element characteristic mode analysis, the following key findings were obtained: The normalized frequency V of the step-index multimode fiber (20 μm core, $\Delta n = 0.004$) is much greater than 2.4048, indicating the transmission of multiple higher-order modes. The effective refractive index, n_{eff}, lies between 1.444 and

1.448, and the mode field distribution exhibits a clear radial oscillatory structure. Calculations of the power-limiting factor for double-clad fiber show that this parameter increases significantly with increasing effective mode refractive index: when neff increases from 1.4439 to 1.4478, the Γ value increases from 14.25% to 96.49%, indicating that higher-order modes have stronger core-power-constraint capabilities. However, in practical fiber amplifier design, a trade-off between this and beam quality must be considered. At a bending radius of 10 cm, the fiber mode field exhibits a significant asymmetric distribution, with the peak electric field shifting outward from the bend and a leakage field appearing in the cladding. A slight decrease in effective refractive index (1.4498-1.4511) indicates that bending introduces an equivalent refractive index perturbation, weakening the mode confinement capability. Compared with conventional step-index fibers, microstructured fibers, due to their high refractive-index contrast and structural confinement, exhibit superior mode-field stability and bending resistance under the same bending conditions. By introducing a PML and an SBC, the leakage mode characteristics of the microstructured fiber were successfully simulated. The change in the imaginary part of n_{eff} from 2.1612×10^{-5i} to 1.9981×10^{-5i} indicates that even small perturbations can significantly affect leakage loss, reflecting the high sensitivity of this structure to external perturbations such as temperature and stress. The asymmetric distribution and local enhancement of the magnetic field component |Hy| around the air hole further verify the modulation effect of the high refractive-index contrast on the field distribution. The COMSOL-based coupling analysis framework offers several advantages: First, it enables the coordinated solution of electromagnetic, thermal, and stress fields, fully capturing the influence of thermo-optical and elasto-optical effects on mode characteristics. Second, through parametric scanning and adaptive mesh refinement, it ensures the computational accuracy of key indicators such as bending loss and confinement factor. Third, its visualization capabilities intuitively reveal the microscopic mechanisms of mode field distortion, energy leakage, and multi-field coupling. This research provides important insights for the design of next-generation optical fibers, including improving bending resistance in communication fibers by optimizing refractive index distribution or introducing microstructure units, balancing power limiting factor and mode purity in high-power fiber lasers by rationally designing core diameter and inner cladding size, and improving detection sensitivity in sensing fibers by utilizing the high sensitivity of microstructures to disturbances and suppressing temperature crosstalk through thermo-optical compensation design. Future work will further extend to dynamic multi-field coupling scenarios, exploring the evolution of fiber performance under femtosecond laser pulses, thermal shock, and radiation environments.

Authors' Contributions

Khan Rajib Hossain, Investigation, Resources, Data curation, Writing-Original draft preparation; Md. Auria Hossain, Khan Md Salman Adib Fuad, Muntaha Mahin, Mir Abdul

Gaffar, Md Mehedi Hasan, Jarin Tasnim, Md Rahamatolla, Md Tajul Islam, H M Jahidul Kabir: Resources, writing-reviewing; Md Abdul Jalil: Supervision, Writing- Reviewing and Editing.

Declaration of competing interest

The authors affirm that they have no known financial or interpersonal conflicts that would have appeared to impact the research presented in this study.

Funding

This research did not receive any specific grant from funding agencies in the public, commercial, or not-for-profit sectors.

Ethical Approval

This article does not contain any studies involving human participants or animals performed by any of the authors. Therefore, ethical approval was not required.

Consent to Participate

This study did not involve human participants; therefore, informed consent was not required.

Consent to Publish

Not applicable**.**

Data Availability Statement

The data supporting the findings of this study are available from the corresponding author upon reasonable request.

References

1. Faltas, S. (1988). The invention of fibre-optic communications. History and Technology, an International Journal, 5(1), 31-49. https://doi.org/10.1080/07341518808581724.
2. Gangopadhyay, T. K. (2019). Historical facts toward introduction of fiber-optics and photonics. In Photonics and Fiber Optics (pp. 1-37). CRC Press. https://doi.org/10.1201/9780429026584.
3. Moore, N. W., Dominguez, D., Fox, B. P., Ampleford, D. J., Schaeuble, M. A., & Coverdale, C. A. (2025). Thermo-optic and photoelastic effects on fiber optic interferometry during pulsed plasma radiation. Physics of Plasmas, 32(11). https://doi.org/10.1063/5.0294664.
4. Richardson, D. J., Nilsson, J., & Clarkson, W. A. (2010). High power fiber lasers: current status and future perspectives. Journal of the optical society of America B, 27(11), B63-B92. https://doi.org/10.1364/JOSAB.27.000B63.
5. Ma, Y., Wan, R., Li, S., Yang, L., & Wang, P. (2022). Advances in silica-based large mode area and polarization-maintaining photonic crystal fiber research. Materials, 15(4), 1558. https://doi.org/10.3390/ma15041558.
6. ZHANG Y, TAN F, XIE G, GAO B, MU W, (2024). Structural design and performance analysis of wide-band and large-mode-field double cladding photonic crystal fiber. Journal of Applied Optics, 45(4): 865-872. https://dx.doi.org/10.5768/JAO202445.0408001.
7. Liu, Q., Xing, P., Sun, Y., Yao, X., Sun, G., Lv, J., ... & Liu, C. (2025). Study on ultra-low loss hollow-core anti-resonant fiber. https://doi.org/10.1364/opticaopen.29908004.
8. Simović, A., Drljača, B., Kovačević, M. S., Kuzmanović, L., Djordjevich, A., Aidinis, K., ... & Savović, S. (2025). High bandwidth performance of newly designed multimode W-type microstructured plastic optical fibers with graded-index core distribution. Scientific Reports, 15(1), 17108. https://doi.org/10.1038/s41598-025-01411-6.

9. Gopalakrishnan, J., Grosek, J., Pinochet-Soto, G., & VandenBerge, P. (2025). Adaptive resolution of fine scales in modes of microstructured optical fibers. SIAM Journal on Scientific Computing, 47(1), B108-B130. https://doi.org/10.1137/24M1651605.
10. Muduli, N., & Padhy, H. K. (2016). An optimized configuration of large mode field area PMMA photonic crystal fiber with low bending loss: a new approach. Journal of Materials Science: Materials in Electronics, 27(2), 1906-1912. https://doi.org/10.1007/s10854-015-3972-5.
11. Gan, J., Yang, A., Guo, Q., & Yang, Z. (2024). Flexible optical fiber sensing: materials, methodologies, and applications. Advanced Devices & Instrumentation, 5, 0046. https://doi.org/10.34133/adi.0046.
12. Yariv, Amnon, and Pochi Yeh. (2007). Photonics: Optical Electronics in Modern Communications (version Public Access - front matter, author index, subject index). 6th ed. Oxford, UK: Oxford University Press.
13. Yadgeer, S. A., Ray, S., & Joglekar, P. V. (2023, February). Study of chromatic dispersion in single-mode optical fiber. In Journal of Physics: Conference Series (Vol. 2426, No. 1, p. 012026). IOP Publishing. https://doi.org/10.1088/1742-6596/2426/1/012026.
14. Zhang, J., Fang, H., Wang, P., Fang, W., Zhang, L., Guo, X., & Tong, L. (2024). Optical microfiber or nanofiber: a miniature fiber-optic platform for nanophotonics. Photonics Insights, 3(1), R02-R02. https://doi.org/10.3788/PI.2024.R02.
15. Li, L., & Qing-chao, S. (2025). Research on novel variable air-hole photonic crystal fiber. Journal of Optical Communications, 46(1), 135-139. https://doi.org/10.1515/joc-2022-0099.
16. Hou, S., & Han, J. (2010). The fabrication tolerances and mode mechanism of a microstructured fiber for broadband dispersion-compensating with low nonlinearity. Optical Fiber Technology, 16(5), 315-317. https://doi.org/10.1016/j.yofte.2010.08.005.
17. Tenderenda, T., Szostkiewicz, L., Stanczyk, T., Bienkowska, B., Kunicki, D., Murawski, M., ... & Nasilowski, T. (2017). Analysis of phase sensitivity to longitudinal strain in microstructured optical fibers. Optics express, 25(11), 12216-12221. http://dx.doi.org/10.1364/oe.25.012216.
18. Wray, J. H., & Neu, J. T. (1969). Refractive index of several glasses as a function of wavelength and temperature. Journal of the optical Society of America, 59(6), 774-776. https://doi.org/10.1364/JOSA.59.000774.
19. Malitson, I. H. (1965). Interspecimen comparison of the refractive index of fused silica. Journal of the optical society of America, 55(10), 1205-1209. https://doi.org/10.1364/JOSA.55.001205.
20. Touloukian, Y. S., Kirby, R. K., Taylor, E. R., & Lee, T. Y. R. (1977). Thermophysical properties of matter-the tprc data series. volume 13. thermal expansion-nonmetallic solids.
21. Jameel, R. T., & Salih, A. R. (2026). Calculating the Linearly Polarized Modes and their Properties in Weakly Guiding Step Index Fibers. Ibn AL-Haitham Journal For Pure and Applied Sciences, 39(1), 108-117. https://doi.org/10.30526/39.1.4166
22. Wang, Z., Geng, W., Zhao, W., Zeng, Z., Liu, Y., Peng, Q., ... & Yue, Y. (2025). Graded-index coupled ring-core fiber for highly dispersive and high-purity OAM modes. Physics Letters A, 130951. https://doi.org/10.1016/j.physleta.2025.130951.
23. Gloge, D. (1971). Weakly guiding fibers. Applied optics, 10(10), 2252-2258. https://doi.org/10.1364/AO.10.002252.

24. Keiser, G. (2021). Fiber optic communication networks. In Fiber Optic Communications (pp. 507-575). Singapore: Springer Singapore. https://doi.org/10.1007/978-981-33-4665-9_13.
25. Agrawal, G. P. (2012). Fiber-optic communication systems. John Wiley & Sons.
26. Kadhim, A. A., & Salih, A. R. (2025, June). Calculating the Modes Properties for Step-Index Multimode Optical Fibers at Nd: YAG Laser Wavelength. In Journal of Physics: Conference Series (Vol. 3028, No. 1, p. 012030). IOP Publishing. https://doi.org/10.1088/1742-6596/3028/1/012030.
27. Pryamikov, A. D., Alagashev, G. K., Kosolapov, A. F., & Biriukov, A. S. (2016). Impact of core-cladding boundary shape on the waveguide properties of hollow core microstructured fibers. Laser Physics, 26(12), 125104. https://doi.org/10.1088/1054-660X/26/12/125104.
28. Liang, J., Yonggang, Z., Ye, D., He'nan, C., Li, X., & Xiaohui, M. (2013). Research and optimization on refractive index and core of double cladding fiber. High Power Laser and Particle Beams, 25(10), 2496-2500. https://doi.org/10.3788/HPLPB20132510.2496.
29. Qirong, X., Haicui, R., Xiao, C., Ping, Y., & Mali, G. (2014). Research on characteristics of co-linear side-pumping couplers with special double-clad fibers. Journal of Modern Optics, 61(4), 307-314. https://doi.org/10.1080/09500340.2014.884652.
30. Berenger, J. P. (1994). A perfectly matched layer for the absorption of electromagnetic waves. Journal of computational physics, 114(2), 185-200. https://doi.org/10.1006/jcph.1994.1159.
31. Bertholds, A., & Dandliker, R. (2002). Determination of the individual strain-optic coefficients in single-mode optical fibres. Journal of lightwave technology, 6(1), 17-20. https://doi.org/10.1109/50.3956.